

Los Alamos National Laboratory is operated by the University of California for the United States Department of Energy under contract W-7405-ENG-82

TITLE
Ringwaldmania Reconsidered

AUTHOR(S)
Michael P. Mattis
Theoretical Division T-8
Los Alamos National Laboratory
Los Alamos, NM 87545

SUBMITTED TO
Proceedings of the International Workshop for
Electroweak Symmetry Breaking Nov. 12 - 15, 1991
Hiroshima, ed. by. T. Muta

DISCLAIMER

This report was prepared as an account of work sponsored by an agency of the United States Government. Neither the United States Government nor any agency thereof nor any of their employees, makes any warranty, express or implied, or assumes any legal liability or responsibility for the accuracy, completeness, or usefulness of any information, apparatus, product, or process disclosed, or represents that its use would not infringe privately owned rights. Reference herein to any specific commercial product, process, or service by trade name, trademark, manufacturer, or otherwise, does not necessarily constitute or imply its endorsement, recommendation, or approval by the United States Government or any agency thereof. The views and opinions of authors expressed herein do not necessarily state or reflect those of the United States Government or any agency thereof.

In accordance with this notice, the publisher recognizes that the U.S. Government retains a nonexclusive, irrevocable, and exclusive right in and to the copyright in this article to allow others to do so for U.S. Government purposes.

The Los Alamos National Laboratory requests that the publisher identify this article as work performed under the auspices of the U.S. Department of Energy.

Los Alamos Los Alamos National Laboratory,
Los Alamos, New Mexico 87545



Ringwaldmania Reconsidered

MICHAEL P. MATTIS[†]

*Theoretical Division T-8, Los Alamos National Laboratory
Los Alamos, NM 87545*

The exciting possibility that anomalous baryon and lepton number violation might be observable at the next generation of supercolliders is suggested by an instanton calculation due to Ringwald and Espinosa. Here, the current controversial status of these claims is discussed, and progress on several fronts is described.

INTRODUCTION. Over two years ago, a startling calculation by Ringwald^[1] and later Espinosa^[2] suggested the *possibility* that anomalous baryon and lepton number (B and L) violation in the Standard Model *might* be observable at the upcoming generation of supercolliders. From the start, the reaction among theorists has run the gamut from unbridled optimism to extreme skepticism. Remarkably, theorists today appear no closer to a consensus on this issue, but at least the main field-theoretic issues are in much sharper focus. In this brief review, I will sketch some of the recent progress in the field, with unabashed emphasis on my own recent work.^[3,4] For reasons of space, much of what follows will necessarily be in "journalistic mode"; those readers desiring more details are referred to the much more thoroughgoing review, Ref. [5].

The inclusive $2 - n$ processes one has in mind are of the form

$$q + q \rightarrow 3\bar{q} + 3\bar{l} + n_w * W + n_z * Z + n_h * \phi, \quad (1)$$

where q and l stand for quarks and leptons, and n_w , n_z and n_h are the numbers of W 's, Z 's and Higgs bosons created. Note that B and L are each violated by three units, as required by the chiral anomaly. At low energies, the dominant boson multiplicities (n_w, n_z, n_h) are small, and the inclusive B -violating cross section $\sigma_B \sim e^{-2\pi/\alpha_w}$, with $\alpha_w = g_w^2/4\pi \approx 0.3$. This is the typical exponential suppression

[†] Supported by a J. R. Oppenheimer Fellowship. Internet: mattis@prod.lanl.gov

associated with instanton-mediated tunneling. But at high energies, $\langle n_W \rangle$ are enormous, of order π/α_w , and the tunneling suppression is *potentially* compensated by the exponentially large phase space available for producing so many low-energy (“soft”) bosons, leaving an unsuppressed net result for σ_B .^[6] More concretely, one can show^[7]

$$\sigma_B \sim \exp \left\{ \frac{4\pi}{\alpha_w} \left[-1 + \frac{1}{2} (3\epsilon)^{4/3} + \mathcal{O}(\epsilon^{6/3}) \right] \right\}, \quad \epsilon = \frac{\alpha_w E}{4\pi M_W}. \quad (2)$$

So the characteristic energy at which the tunneling suppression might be overcome is the sphaleron scale $E_{\text{sphal}} \sim \pi M_W/\alpha_w \approx 10$ TeV, the typical scale for nonperturbative physics in Electroweak theory.

Pictorially, the Ringwald-Espinoza calculation is depicted in Fig. 1. Unfortunately, as these authors both acknowledged, their naive instanton calculation breaks down long before the energy approaches the interesting range of the sphaleron. Subsequently, much progress has been made towards classifying the corrections to their calculation. The important corrections are presently understood to fall into three major categories:

(i) **Final-state corrections**^[6–11] (Fig. 2) can be treated semiclassically, through the construct of *distorted instantons*. Numerically, they tame the rise of σ_B and ensure that the unitarity bound is not violated.^[11] We will review the “valley method” for summing final-state corrections,^[11,12] and discuss the possibility^[3] that *bifurcations* in the valley cause a nonanalytic halt to the smooth exponential rise of σ_B towards an observably large value.

(ii) **Initial-state corrections**^[13,14] (Fig. 3) are those involving the high-energy (“hard”) incoming quanta. Unlike final-state corrections which are characterized by tree graphs and so can be treated semiclassically, initial-state corrections are intrinsically quantum effects: that is, they are dominated by graphs containing enormous numbers (order $1/g^2$) of loops. From a calculational point of view, this fact would appear to be extremely discouraging. Nevertheless, we shall see that — despite the importance of loops — the hard line corrections, looked at in the right way, might be treatable *semiclassically*, that is, by *tree graphs alone*.^[4]

(iii) **Multi-instanton corrections**^[15–17] (Fig. 4) become important, by definition, when the dilute instanton gas approximation breaks down. Whether this occurs *before*^[16,17] or *after*^[15,18] the one-instanton result has a chance to grow large is currently a hotly debated question, reviewed below.

Let us now delve a little further into each of these three topics.

FINAL-STATE CORRECTIONS To understand why it is that the backreaction of the large number of final-state quanta produced in the process (1) *must* distort the instanton, consider the trivial analogy of a one-dimensional integral

$$J_0 = \int dx e^{S(x)} \quad (3)$$

for some generic complex function S . In the limit of small α , the leading exponential behavior of \mathcal{A}_0 will be given by

$$\mathcal{A}_0 \sim e^{S(x_0)/\alpha} \quad (4)$$

where x_0 is the complex saddle-point of S , and we are ignoring inessentials such as Gaussian prefactors. Likewise, to this approximation, an n th moment of this integral will be simply given by

$$\mathcal{A}_n \equiv \int dx x^n e^{S(x)/\alpha} \sim x_0^n e^{S(x_0)/\alpha} \quad (5)$$

However, what if n is not held fixed as $\alpha \rightarrow 0$, but is itself scaling like $1/\alpha$? Then Eq. (5) is no longer valid. Instead, one should rewrite x^n as $e^{n \log x}$, and solve for the new saddle-point x'_0 by extremizing the full exponent including the logarithm. The analogy to n -point functions in quantum field theory is clear: x_0 represents the usual zero-energy instanton, n (or rather, $n - 2$) is the multiplicity of final-state particles, and x'_0 is the *distorted* instanton including their effect.

How to solve for the distorted instanton? In practice, the best way is with the help of the optical theorem: one extracts the imaginary part of a *nonanomalous* $2 \rightarrow 2$ forward scattering amplitude, restricting attention to intermediate states comprising an instanton-antiinstanton ($I\bar{I}$) pair (see Fig. 5).^[7,11] The $I\bar{I}$ attraction leads inevitably to their cigar-shaped distortion along the axis of their separation. This distortion is governed by a *classical* equation of motion, the so-called valley equation,^[12] whose solution is formally equivalent^[19] to summing the infinite set of final-state trees such as Fig. 2. The valley equation is simply the Euler-Lagrange equation subject to a set of Faddeev-Popov constraints on the quasi-zero-modes of the problem, namely the scale sizes ρ_I and $\rho_{\bar{I}}$, relative separation R , and global isospin orientations of I and \bar{I} , and with the boundary condition that as $R \rightarrow \infty$, I and \bar{I} relax to their usual zero-energy undistorted form. On general grounds, the “valley” configurations which solve this equation interpolate smoothly between this long-distance boundary condition on one end of parameter space, and the perturbative vacuum on the other end as $R \rightarrow 0$ and I and \bar{I} annihilate.^[12]

Unfortunately, the exact form of the valley is unknown in Electroweak theory, due to the dimensionful Higgs VEV v , but in pure Yang-Mills theory, which is conformally invariant, it is.^[12] Given knowledge of the Yang-Mills valley, Khoze and Ringwald have proposed an interesting toy model for B violation in Electroweak theory which we now review. The Khoze-Ringwald model is summarized by the following expression^[14],

$$\tau_B \sim \text{Im} \int dR d\rho_I d\rho_{\bar{I}} \exp \{ ER - S_{\text{val}}(\rho_I, \rho_{\bar{I}}, R) - \tau^2 (\rho_I^2 + \rho_{\bar{I}}^2) v^2 \} \quad (6)$$

Here the integration runs over the relevant quasi-zero modes $\{\rho_I, \rho_{\bar{I}}, R\}$ of the $I\bar{I}$ system. The three terms in the exponent have the following meaning. The first

is due to the *initial*-state quanta, whose effects are otherwise suppressed in this model. This term is the Euclidean continuation of the initial-state phase factor $e^{-iP_{\text{tot}} \cdot x_i} e^{iP_{\text{tot}} \cdot x_f}$, where x_I ($x_{\bar{I}}$) is the center of the (anti)instanton, $R = x_I - x_{\bar{I}}$, and the total $+$ -momentum of the system P_{tot} is taken in the center of mass frame, $P_{\text{tot}} = (E, \mathbf{0})$. The second term, S_{val} , is the Euclidean action for the Yang-Mills $I\bar{I}$ valley.^[12] The third term is an infrared cutoff on large-size (anti)instantons due to the Higgs,^[20,21] whose degrees of freedom are otherwise ignored.

We wish to estimate this integral in the limit $g^2 \rightarrow 0$ with E/E_{min} fixed. In this regime, the dominant values of ρ_I , $\rho_{\bar{I}}$ and R are expected to scale like^[6] M_W^{-1} , so that an overall factor of g^{-2} factors smoothly out of all three terms in the exponent of Eq. (6). The integral is then ripe for a saddle-point analysis. It is easy to show that $\rho_I = \rho_{\bar{I}} \equiv \rho$ at the saddlepoint.^[10,11] Switching to dimensionless variables $\chi = R/\rho$, $\xi = gv\rho/2$ and ϵ as in Eq. (2), we can rewrite the exponent as:^[11]

$$\frac{4\pi}{\alpha_w} \Gamma = \frac{4\pi}{\alpha_w} \left\{ \epsilon \chi \xi - \bar{S}(\chi) - \frac{1}{2} \xi^2 \right\} \quad (7)$$

where the rescaled action $\bar{S} = \alpha_w S_{\text{val}}/4\pi$ is a g -independent function of χ only. The saddle-point equations read

$$0 = \frac{\partial \Gamma}{\partial \xi} = \epsilon \chi - \xi, \quad 0 = \frac{\partial \Gamma}{\partial \chi} = \epsilon \xi - \bar{S}'(\chi). \quad (8)$$

Eliminating ξ then leaves

$$\epsilon^2 \chi = \bar{S}'(\chi). \quad (9)$$

As seen in Fig. 6, Eq. (9) can be solved graphically for the stationary value of χ , which we shall call χ_* , as a function of ϵ . For large $I\bar{I}$ separations, one can show^[12]

$$\bar{S}(\chi) \underset{\chi \rightarrow \infty}{\sim} 1 - \frac{6}{\chi^4} + \mathcal{O}(\chi^{-6}), \quad (10)$$

the first term on the right-hand side being just twice the rescaled instanton action. In this limit, Eq. (9) becomes $\epsilon^2 \chi_* \simeq 24/\chi_*^3$ so that

$$\chi_* \simeq \left(\frac{24}{\epsilon^2} \right)^{1/3}, \quad \xi_* \simeq (24\epsilon^4)^{1/3}. \quad (11)$$

We then recover the leading exponential growth of σ_B , Eq. (2), from (7), (10) and (11). Note that large χ corresponds to low energy.

Conversely, as energy increases, χ_* tends to zero, hence ξ_* , and indeed the full exponent Γ tend to zero as well, and σ_B overcomes its exponential suppression. This phenomenon happens, not asymptotically as $\epsilon \rightarrow \infty$, as one might think, but

rather at a *finite* critical energy ϵ_{crit} , which is the energy for which the dashed line in Fig. 6 is tangent to the curve. Eq. (9) allows us to solve for ϵ_{crit} :

$$\epsilon_{\text{crit}} = \sqrt{\tilde{S}''(0)}. \quad (12)$$

For the particular valley action used by Khoze and Ringwald, one finds $\tilde{S}(\chi) = \frac{6}{5}\chi^2 - \frac{4}{3}\chi^3 + \dots$ so that σ_B sheds its exponential suppression when $\epsilon_{\text{crit}} = \sqrt{12/5}$, i.e., $E \approx 40$ TeV, beyond the range of SSC but still formally of order E_{vphal} , and therefore of great interest to theorists.

How *robust* is the Khoze-Ringwald model? That is, to what extent are its optimistic conclusions toy-model-independent? On this question, the jury is still out. To pinpoint a potential problem,^[3] let us ponder the first-principles behavior of the action as $\chi \rightarrow 0$. In this limit, the valley collapses into the perturbative vacuum, which implies $\tilde{S}(0) = 0$, while stability of the perturbative vacuum further implies that $\tilde{S}'(0) = 0$ and $\tilde{S}''(0) > 0$. However, we know of no general principle governing the sign of the *third* derivative $\tilde{S}'''(0)$! Accordingly, let us consider a seemingly minor modification of Fig. 6, one in which $\tilde{S}'''(\chi)$ is positive rather than negative, as shown in Fig. 7. There are now *two* critical energies in the problem, ϵ_1 and ϵ_2 . For $\epsilon < \epsilon_1$, there are two solutions as before, the perturbative vacuum at $\chi = 0$, and the B -violating solution at large χ . Starting at $\epsilon = \epsilon_1$, a third solution to Eq. (9) is born out of the perturbative vacuum. As ϵ is then increased to ϵ_2 , this middle root migrates outward towards the far root: they coalesce precisely when $\epsilon = \epsilon_2$. For still larger energies, these two roots split off into complex conjugate pairs. The B -violating solution can then be said to have *bifurcated*: the perturbative vacuum is probably never reached; and presumably σ_B always remains exponentially suppressed^[3]

In light of this pessimistic scenario, how does one decide on physical grounds whether it is Fig. 6 or Fig. 7 that is relevant? I would claim, *one can't*. The reason is that the valley itself, and hence the valley action as a function of the collective coordinates, is not a well-defined concept:^[12] it depends on how one chooses to implement the Faddeev-Popov procedure, i.e., on the "weight function" on configuration space that one uses in solving the valley equation. In Ref. [3], it is demonstrated (at least for generalized Khoze-Ringwald models, if not necessarily for the true Electroweak valley which is unknown) that *different choices of weight functions allow one to switch at will between the two scenarios, Fig. 6 and Fig. 7*

Of course, measurable physical quantities such as cross sections cannot depend on mathematical conventions such as one's choice of weight function. The resolution of this apparent paradox is the following. The valley method only deals with a *piece* of the total problem, the final-state corrections. Once the corrections involving the high-energy initial-state particles are added in, the total answer will indeed be independent of weight function^[12, 19]. So, the initial-state corrections truly cannot be avoided, and it is to these that we next turn our attention.

INITIAL-STATE CORRECTIONS. The importance of initial-state corrections to the problem of B violation was driven home by a surprising calculation due to Mueller.^[13] He examined propagators $G(p, q)$ in the instanton background, in the relevant kinematic regime where $p \cdot q \sim (E_{\text{max}})^2$ while p^2 and $q^2 \sim M_W^2$. The result is that the ratio of the ostensibly perturbative propagator correction, Fig. 8b, to the Ringwald approximation to the 2-point function shown in Fig. 8a, goes like $\alpha_w p \cdot q M_W^{-2}$. Therefore, rather than being smaller by a factor of α_w , Fig. 8b is actually *bigger* by a factor of $1/\alpha_w$. Furthermore, corrections involving loops such as Fig. 8c are bigger still, dominating Fig. 8a by a factor of $\alpha_w^{-(l+1)}$, l being the number of loops. The dominant loop graphs turn out to be of a special type: they can all be pictured as *squared trees* in which the leaves from each tree are tied together in all possible ways. Similar statements hold for 3- and higher-point functions as well.

Let us admit the following: If a believable estimate for σ_B truly requires an accurate evaluation of complicated multiloop diagrams, then the problem is hopeless. The reason is that it will not be *semiclassical*: there will exist no classical equation that can be fed to a computer with appropriate boundary conditions, whose solution will give the leading exponential behavior of σ_B . (Remember that classical equations only sum tree graphs.) Conversely, if the problem of high-energy B violation can ultimately be solved, it must be the case that Mueller's loops, looked at the right way, can be reproduced by tree graphs alone. I will now review a promising indication that this is, in fact, the case.^[4]

For convenience, in order to isolate the effect of high-energy lines, we will not allow the multiplicity to grow large. Instead, let us focus on an *exclusive* process, say $2 \rightarrow 3$ as pictured in Figs. 9-11, in the limit that a lot of energy has been pumped into the system, so that all the $p_i \cdot p_j \gg M_W^2$, $i \neq j$. The associated 5-point function, treated in Ringwald approximation, is shown in Fig. 9; the leading and subleading "corrections" (actually, as already noted, they are bigger than Fig. 9) are shown in Figs. 10 and 11, respectively. For explicit formulae corresponding to these figures, the reader is referred to Ref. [13]; the important point emphasized by Mueller is that loops and trees conspire to give a relatively simple result.

Now let us repeat this calculation in a different, and seemingly more awkward way, using an effective action approach.^[4] We evaluate the n -point function

$$\int DA A^{\mu_1 \nu_1}(p_1) \dots A^{\mu_n \nu_n}(p_n) e^{iS[A]} \quad (13)$$

by splitting the fields into classical and fluctuating components, and making the replacement

$$A^{\mu_i \nu_i}(p_i) = A_{\text{inst}}^{\mu_i \nu_i}(p_i) + \delta A^{\mu_i \nu_i}(p_i) = A_{\text{inst}}^{\mu_i \nu_i}(p_i) \exp \log \left(1 + \frac{\delta A^{\mu_i \nu_i}(p_i)}{A_{\text{inst}}^{\mu_i \nu_i}(p_i)} \right) \quad (14)$$

Taylor expanding the logarithms then leads to an infinite number of new interaction vertices which we shall denote graphically by thick blobs. Other vertices come from

the usual action $S[A]$ which we likewise expand about A_{inst} . Note that unlike usual vertices, m -point blobs $\sim g^m$ from $(A_{\text{inst}})^{-m}$. Another difference is that blobs are real whereas the usual vertices come with the standard factor of i attached. Finally, they are local in momentum-space, not position-space. Evaluating the n -point function (13) now becomes equivalent to calculating the effective action in the presence of the new interactions generated by

$$\sum_{i=1}^n \log \left(1 + \frac{\delta A^{\mu_1 \dots \mu_n}(p_i)}{A_{\text{inst}}^{\mu_1 \dots \mu_n}(p_i)} \right), \quad (15)$$

and exponentiating the result. The contributions to the effective action analogous to Figs. 10 and 11 are pictured in Figs. 12 and 13, respectively.

Of course, if carried out *exactly*, both calculational methods must precisely agree. The nontrivial observation is this:^[4] If, following Mueller, one only keeps terms contributing to the leading exponential behavior of σ_B , then in the effective action approach it suffices to keep the *tree graphs alone*, Figs. 12a, 13a and 13b. Equivalently, the loop contributions to the effective action all cancel to these orders. Granted, this has only been shown explicitly at the one-loop level, but the tentative moral is: despite Mueller's loops, the problem of high-energy B violation appears to be semiclassical after all.

MULTI-INSTANTON CORRECTIONS. Thus far, we have restricted our instanton calculations to the *dilute gas* approximation. That is, we have considered perturbation theory about a single instanton I and neglected III , $IIII$, etc. Indeed, most of the workers in B violation who have speculated on the role of such multi-instanton configurations have assumed that these cannot be significant until such energies that single-instanton amplitudes themselves have gotten observably large (if that ever happens), at which energies the multi-instantons help to unitarize σ_B .^[6,15] This intuition is ingrained from quantum mechanical examples such as the double well, where back-and-forth transitions between the two wells can be neglected until the energy reaches the potential barrier E_{quasi} , which is precisely the point where the one-instanton tunneling amplitude loses its exponential suppression. If this is also the case in field theory, then multi-instantons can be safely ignored for purposes of answering the fundamental question, Does σ_B become observably large at accelerator energies?

In light of this intuition come the surprising claims by Zakharov^[16] and Maggiore and Shifman^[17] (ZMS) that multi-instanton effects become important *long before* the one-instanton amplitude has grown large. The basic argument is easily summarized. ZMS use an effective Lagrangian approach in which (anti)instanton interactions are represented by effective nonrenormalizable multiparticle vertices.^[23] In this language, a forward $2 \rightarrow 2$ amplitude will have multi-instanton contributions such as was shown in Fig. 4. σ_B is then extracted via the optical theorem through appropriate cuttings.

Now attach a tunneling suppression factor of $e^{-2\pi/\alpha_w}$ to each effective vertex, and attach the exponentially growing part of σ_B to each "bond" connecting an I to an \bar{I} . For example, truncating Eq. (2) at the $\epsilon^{4/3}$ order, we would associate the bond with $\exp\left\{\frac{4\pi}{\alpha_w} \cdot \frac{1}{2}(3\epsilon)^{4/3}\right\}$. So the $I\bar{I}$ and $I\bar{I}I\bar{I}$ contributions to σ_B (Fig. 5 and Fig. 4) go like $\exp\left\{\frac{4\pi}{\alpha_w}\left[-1 + \frac{1}{2}(3\epsilon)^{4/3}\right]\right\}$ and $\exp\left\{\frac{4\pi}{\alpha_w}\left[-2 + \frac{3}{2}(3\epsilon)^{4/3}\right]\right\}$, respectively. The simple observation of ZMS is that the latter exponential reaches unity when the former is still tiny, $e^{-4\pi/3\alpha_w}$. In fact, iterating the same bond function, one easily finds that the chain consisting of an infinite number of $I\bar{I}$ pairs reaches unity when the one-instanton result is $e^{-2\pi/\alpha_w}$ —the geometric mean of the few \rightarrow few ($\sim e^{-4\pi/\alpha_w}$) and the many \rightarrow many (~ 1) anomalous cross sections. Obviously this argument is independent of one's choice of bond function, so long as it grows with energy.

What is the consequence of this proposed breakdown of the dilute instanton gas approximation? In principle, the sum of all multi-instanton contributions could be either suppressed or unsuppressed. ZMS guess that they assemble into a geometric series, *e.g.*,

$$\begin{aligned} \sigma_B &\sim \exp\left\{\frac{4\pi}{\alpha_w}\left[-1 + \frac{1}{2}(3\epsilon)^{4/3}\right]\right\} - \exp\left\{\frac{4\pi}{\alpha_w}\left[-2 + \frac{3}{2}(3\epsilon)^{4/3}\right]\right\} \\ &\quad + \exp\left\{\frac{4\pi}{\alpha_w}\left[-3 + \frac{5}{2}(3\epsilon)^{4/3}\right]\right\} - \dots \\ &= \frac{1}{2}e^{-2\pi/\alpha_w} \operatorname{sech}\left\{\frac{2\pi}{\alpha_w}\left[-1 + (3\epsilon)^{4/3}\right]\right\} < e^{-2\pi/\alpha_w}, \end{aligned} \quad (16)$$

in which case B violation is never observable. The alternating signs in (16) presumably come from counting a Gaussian factor of i for each unstable mode of the multi-instanton configuration. If this is eventually confirmed, it would paint a striking picture of the structure of the electroweak vacuum, or at least of the components thereof that couple to high-energy modes: a dense "liquid" of instantons as in QCD, but in stark contrast to QCD, a liquid in which anomalous processes are exponentially suppressed at zero temperature.

The ZMS scenario is intriguing, but at this writing is yet to be bolstered by a compelling calculation. For one thing, it is based on nearest-neighbor two-body interactions, whereas at high energies the typical $I\bar{I}$ separation measured in units of ρ is small, and consequently next-nearest-neighbor as well as three- and higher-body forces should play a role. Furthermore, multi-instanton configurations such as Fig. 4 admit a richer class of tree-graph corrections than does Fig. 5. Finally there is the question of how one cuts these diagrams to reveal purely B -violating amplitudes. Whether, when these issues are all incorporated, it will *still* be true that the multi-instanton contributions catch up to the one-instanton amplitude when the latter is tiny, is a completely open question.

Fortunately, the Khoze-Ringwald model discussed earlier generalizes in a natural way to the case of multi-instantons and so serves as a laboratory for examining the ZMS scenario.^[3] * To proceed, we need to establish one piece of notation. Let us split up the rescaled $I\bar{I}$ valley action \bar{S} from Sec. 2 into an "infinite-distance" piece and a "potential" piece,

$$\bar{S}(\chi) = 1 + V_{I\bar{I}}(\chi). \quad (17)$$

The short- and long-distance boundary conditions on the valley are then $V_{I\bar{I}}(0) = -1$ and $V_{I\bar{I}}(\infty) = 0$.

How to generalize Eq. (17) to the case of $I\bar{I}$ chains such as Fig. 4? Let us go beyond the nearest-neighbor approximation of ZMS (though still preserving the 2-body nature of the interaction for convenience), and postulate a multi-instanton action

$$\bar{S}^{(n)}(\chi) = n + V_{I\bar{I}}^{(n)}(\chi) + V_{I\bar{I}}^{(n)}(\chi) + V_{I\bar{I}}^{(n)}(\chi). \quad (18)$$

Here n denotes the number of $I\bar{I}$ pairs in the chain, and the various 2-body potentials are defined as

$$V_{I\bar{I}}^{(n)}(\chi) = \sum_{k=1}^n (2n - 2k + 1) V_{I\bar{I}}((2k - 1)\chi) \quad (19)$$

and (by $I \leftrightarrow \bar{I}$ symmetry)

$$V_{I\bar{I}}^{(n)}(\chi) = V_{I\bar{I}}^{(n)}(\chi) = \sum_{k=1}^{n-1} (n - k) V_{I\bar{I}}(2k\chi). \quad (20)$$

The sum in Eq. (19) accounts for the $2n - 1$ nearest-neighbor $I\bar{I}$ pairs, the $2n - 3$ next-next-nearest-neighbor $I\bar{I}$ pairs, and so forth, and similarly for Eq. (20). The long-distance boundary condition $\bar{S}^{(n)}(\chi) \rightarrow n$ as $\chi \rightarrow \infty$ is automatically satisfied simply by letting $V_{I\bar{I}}$ and $V_{I\bar{I}} \rightarrow 0$ as $\chi \rightarrow \infty$. Conversely, if the short-distance boundary condition reflecting the collapse of the $I\bar{I}$ chain into the perturbative vacuum, $\bar{S}^{(n)}(\chi) \rightarrow 0$ as $\chi \rightarrow 0$, is to be valid for all n , one requires

$$V_{I\bar{I}}(0) = -V_{I\bar{I}}(0) = 1. \quad (21)$$

We then take as our generalization of the Khoze-Ringwald exponent (7) the following:

$$\Gamma^{(n)} = (2n - 1)\epsilon\chi\xi - \bar{S}^{(n)}(\chi) - \frac{1}{2}n\xi^2. \quad (22)$$

* In what follows, we will ignore the spectra of valley bifurcations raised earlier, the philosophy being that if the single-instanton contribution by itself always remains exponentially suppressed, then the issue of multi-instantons is moot.

The $2n - 1$ multiplying the first term measures the distance in units of R between the endpoints of the chain, assuming an equally-spaced chain for convenience, while the n in front of the third term reflects the additional simplifying assumption that the (anti)instanton scale sizes are all equal.

The critical energies $\epsilon_{\text{crit}}^{(n)}$ at which the n -instanton, n -antiinstanton cross sections $\sigma_{\#}^{(n)}$ overcome their exponential suppression are easily solved for exactly as before, by matching slopes at the origin as per Fig. 6. A few minutes' algebra gives:^[3]

$$\begin{aligned} \epsilon_{\text{crit}}^{(n)} &= \left[\frac{n}{(2n-1)^2} \sum_{k=1}^n \left\{ (2k-1)^2(2n-2k+1)V''_{II}(0) + 8k^2(n-k)V''_{II}(0) \right\} \right]^{1/2} \\ &= \left[\frac{n^3}{3(2n-1)^2} \left((2n^2+1)V''_{II}(0) + (2n^2-2)V''_{II}(0) \right) \right]^{1/2}. \end{aligned} \quad (23)$$

Therefore, assuming non-perverse* choices of $V''_{II}(0)$ and $V''_{\bar{I}\bar{I}}(0)$, the ordering of the critical energies is

$$\epsilon_{\text{anti}}^{(1)} < \epsilon_{\text{anti}}^{(2)} < \epsilon_{\text{anti}}^{(3)} < \dots, \quad (24)$$

which is *precisely reversed* from the ZMS scenario, and consistent instead with the naive intuition that says that multi-instanton contributions can indeed be ignored vis-à-vis the one-instanton sector.

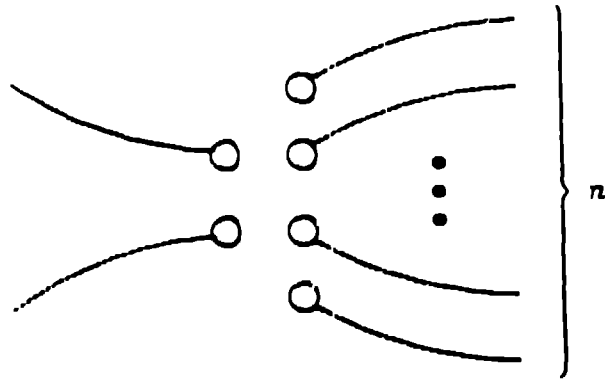
This admittedly toy-model calculation suggests that the ZMS effect is an artifact of the nearest-neighbor approximation. Similar conclusions are reached from the low-energy end by Khoze, Kripfganz and Ringwald.^[18]

In summary, we have examined several current controversies in the study of high-energy B violation, and, in all honesty, have emerged with more incisive questions than decisive answers, to wit: Does the true Electroweak valley bifurcate? Is the process semiclassical? Are multi-instantons important? And of course, the key question that continues to confound us, *Does the B -violating cross section overcome its exponential suppression at a few times the sphaleron energy?*

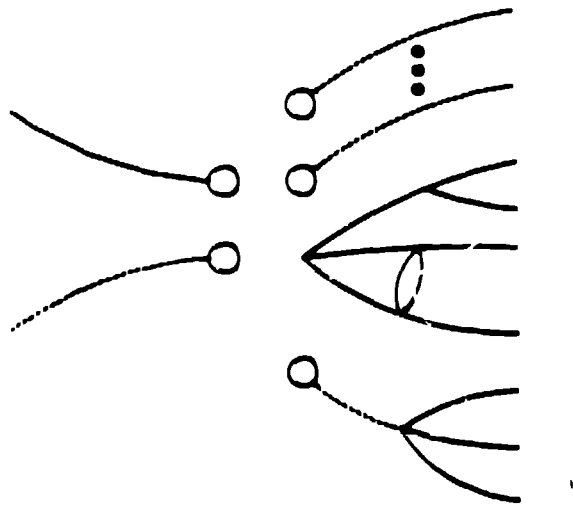
* Requiring that the perturbative vacuum be not only stationary but also stable for all n implies $V''_{II}(0) > 0$ and $V''_{II}(0) + V''_{\bar{I}\bar{I}}(0) \geq 0$, in which case the argument of the square root in (23) is always positive. In the narrow window $-V''_{II}(0) \leq V''_{\bar{I}\bar{I}}(0) < -\frac{13}{18}V''_{II}(0)$, the first inequality in (24) is reversed.

References

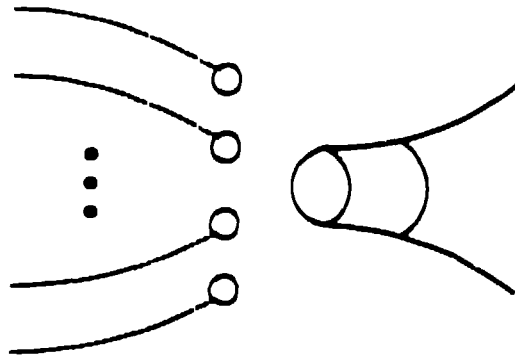
- [1] A. Ringwald, *Nucl. Phys.* **B330**, 1 (1990).
- [2] O. Espinosa, *Nucl. Phys.* **B343**, 310 (1990).
- [3] N. Dorey and M. Mattis, Los Alamos preprint LA-UR-91-3892, *Physics Letters B* (to appear).
- [4] M. Mattis, L. McLerran and L. Yaffe, Washington preprint UW/PT-91-14 (1991).
- [5] M. Mattis, "The Riddle of High-Energy Baryon Number Violation" [revised and expanded version], *Physics Reports* (in press).
- [6] L. McLerran, A. Vainshtein and M. Voloshin, *Phys. Rev.* **D42**, 171, 180 (1990).
- [7] V. Zakharov, TPI preprint TPI-MINN-90/7-T.
- [8] P. Arnold and M. Mattis, *Phys. Rev.* **D42**, 1738 (1990); *Phys. Rev. Lett.* **66**, 13 (1991).
- [9] L. Yaffe, in *Baryon Number Violation at the SSC? Proceedings of the Santa Fe Workshop*, eds. M. Mattis and E. Mottola, Singapore, World Scientific, 1990.
- [10] S. Khlebnikov, V. Rubakov and P. Tinyakov, *Nucl. Phys.* **B350**, 441 (1991).
- [11] V. V. Khoze and A. Ringwald, *Nucl. Phys.* **B355** 351 (1991); *Phys. Lett.* **B259** 106 (1991).
- [12] A. Yung, *Nucl. Phys.* **B297**, 47 (1988); I. Balitsky and A. Yung, *Phys. Lett.* **168B**, 113 (1986).
- [13] A. Mueller, *Nucl. Phys.* **B348**, 310 (1991); *Nucl. Phys.* **B353**, 44 (1991).
- [14] X. Li, L. McLerran, M. Voloshin and R. Wang, TPI preprint TPI-MINN-91/16-T (1991).
- [15] H. Aoyama and H. Kikuchi, *Phys. Lett.* **B247**, 75 (1990); *Phys. Rev.* **D43**, 1999 (1991).
- [16] V. Zakharov, *Nucl. Phys.* **B353**, 683 (1991); Max Planck preprint MPI-PAE/PTh 91-11 (1991).
- [17] M. Maggiore and M. Shifman, TPI preprints TPI-MINN-91/24-T and 91/27-T (1991).
- [18] V. Khoze, J. Kripfganz and A. Ringwald, CERN preprint CERN-TH.6311/91.
- [19] P. Arnold and M. Mattis, *Phys. Rev.* **D44**, 3650 (1991).
- [20] G. 't Hooft, *Phys. Rev.* **D14**, 3432 (1976); **D18**, 2199(E) (1978).
- [21] I. Affleck, *Nucl. Phys.* **B191**, 445 (1981).
- [22] S. Khlebnikov and P. Tinyakov, *Phys. Lett.* **269B**, 149 (1991).
- [23] M. Shifman, A. Vainshtein and V. Zakharov, *Nucl. Phys.* **B165**, 45 (1980).



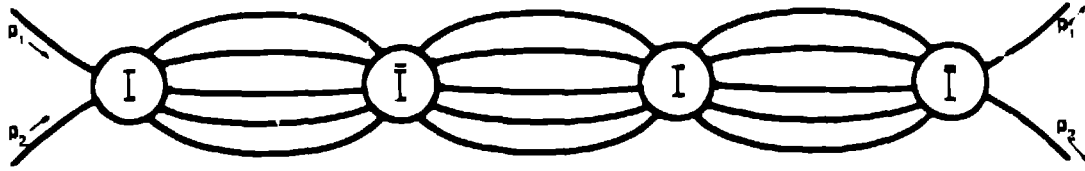
1. A $2 \rightarrow n$ amplitude in "Ringwald approximation," meaning that $\phi \rightarrow \phi_{\text{inst}}$ for each field ϕ in the problem. This substitution is denoted by a dashed line terminating in a circle.



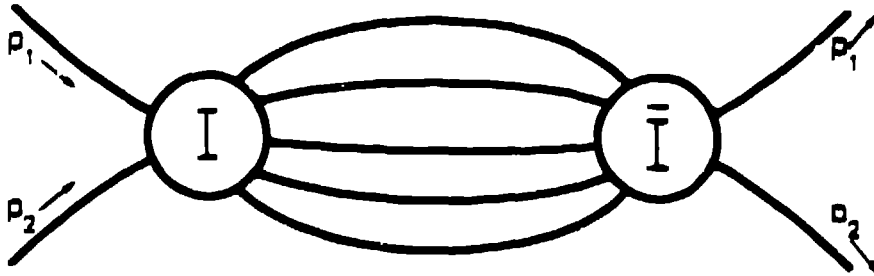
2. A typical final-state correction to Fig. 1. Solid lines henceforth denote propagators in the instanton background.



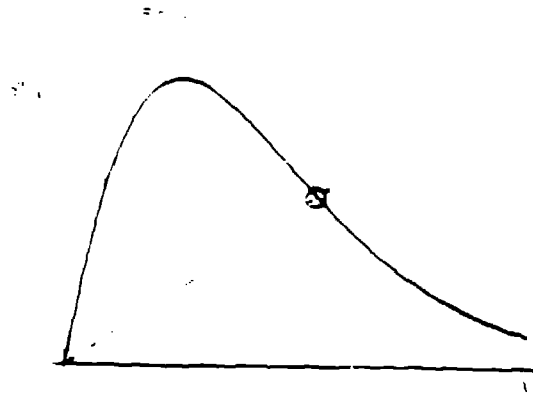
3. A simple initial-state correction to Fig. 1.



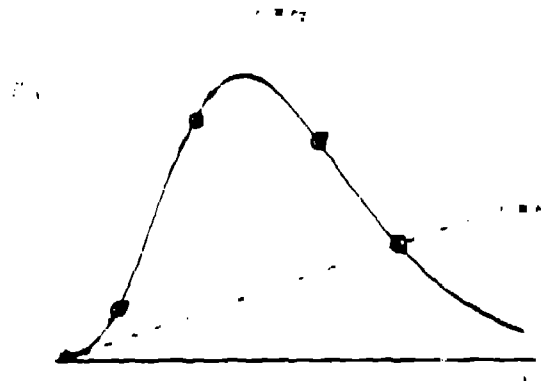
4. A simple multi-instanton chain contribution to a $2 \rightarrow 2$ forward scattering amplitude, which contributes to σ_B via the optical theorem. I (\bar{I}) denote the effective (anti)instanton-induced vertices.



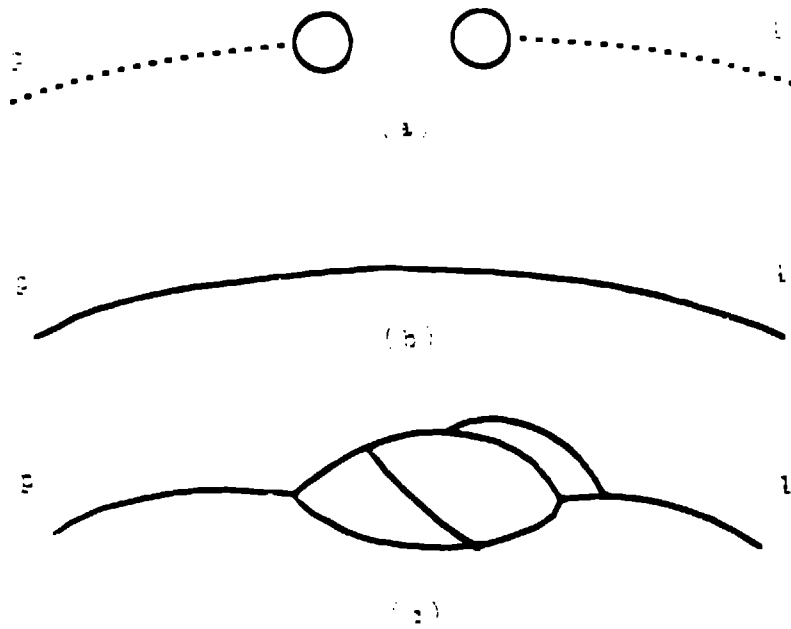
5. A forward scattering amplitude with an $I\bar{I}$ intermediate state.



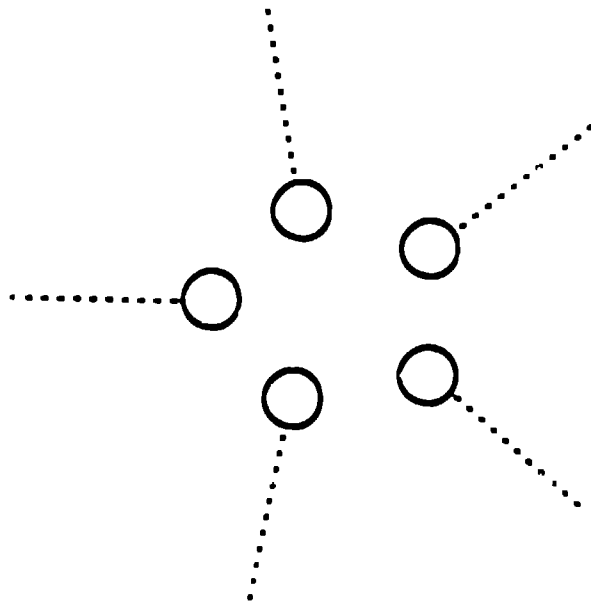
6. The graphical solution of Eq. (9). The slope of the dashed line is the square of the rescaled energy ϵ . σ_B loses its exponential suppression at $\epsilon = \epsilon_{crit}$, where the curves are tangent. For $\epsilon < \epsilon_{crit}$ there are always two roots: the purely B -violating root at $\gamma > 0$, and the perturbative vacuum at $\gamma = 0$. The latter does not contribute to the imaginary part of the amplitude as it is stable, while the former always has precisely one unstable mode which gives a factor of i by analytic continuation.



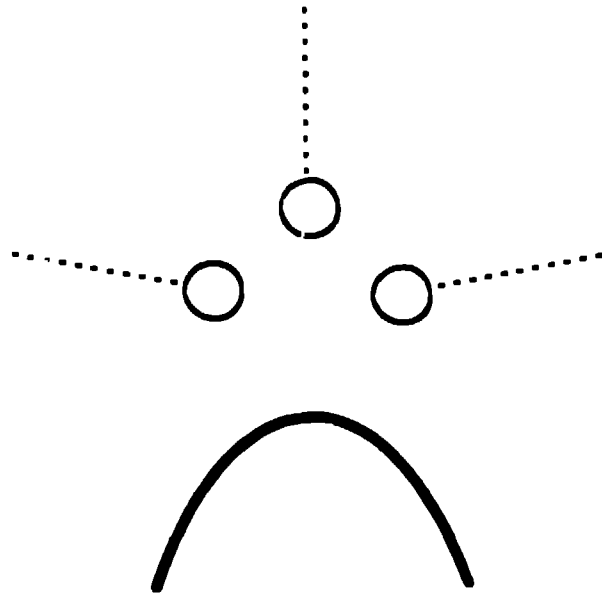
7. A variation of Fig. 6, in which the third derivative of the valley action is now positive at $\gamma = 0$. Now there are two critical energies, ϵ_1 and ϵ_2 , as indicated. See next for discussion.



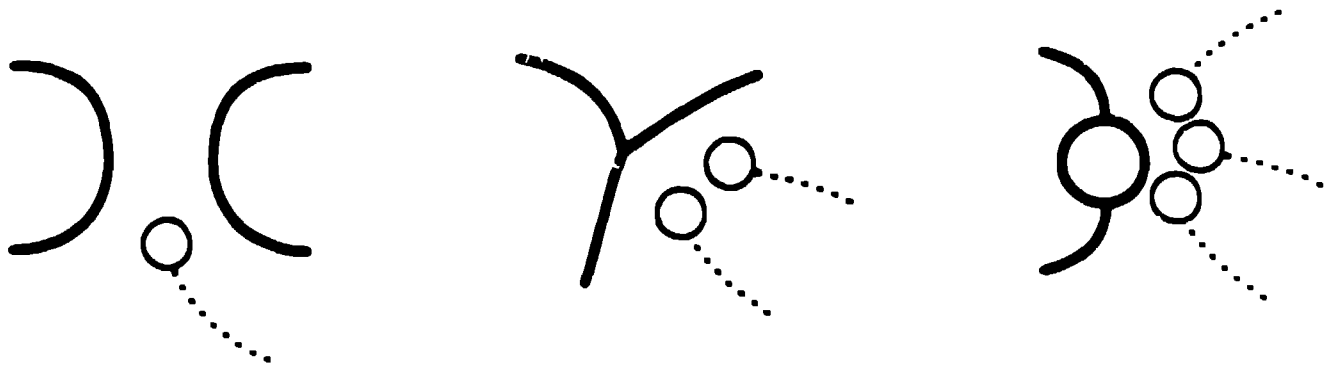
3. Three contributions to the 2-point function. *a.* The 2-point function in Ringwald approximation. *b.* The propagator correction to *a.* *c.* A multi-loop contribution, which can be viewed as a "squared tree" (see text).



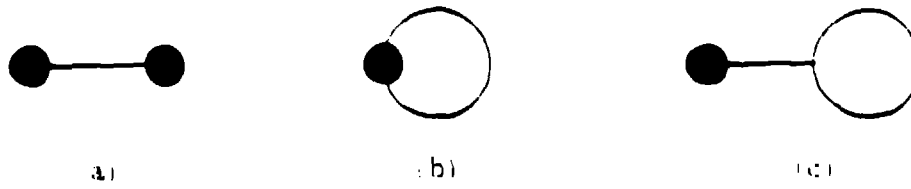
4. A 4-point function in Ringwald approximation.



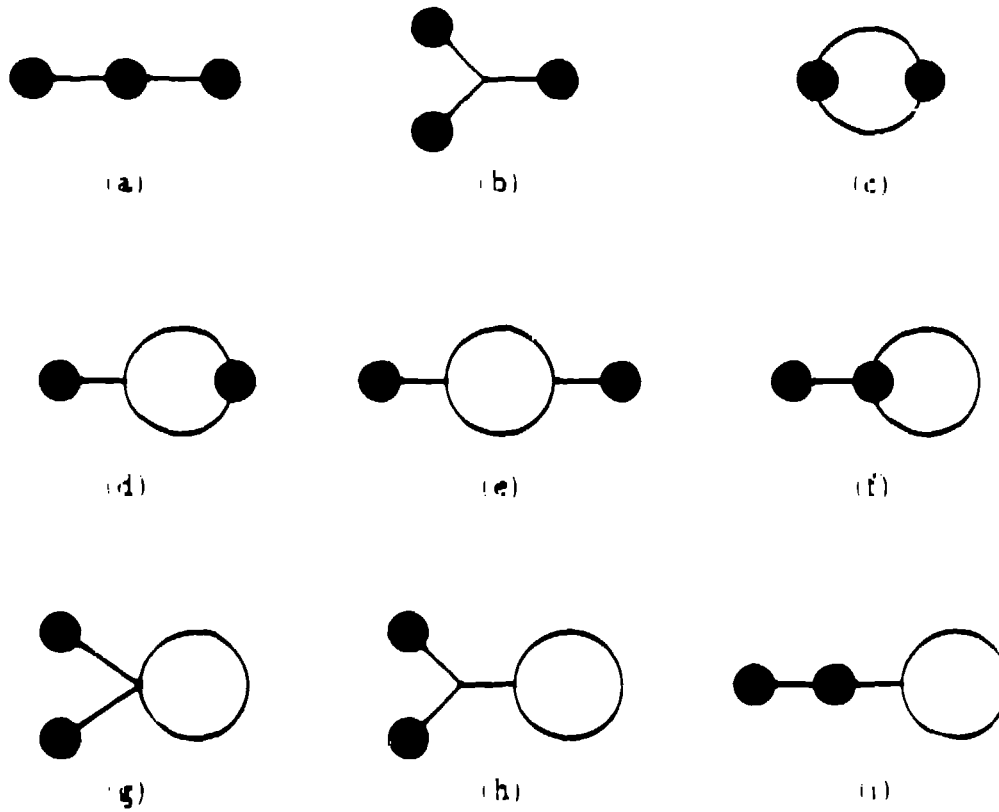
10. The leading $\mathcal{O}(\alpha_w)$ multiplicative contribution to Fig. 9 (since two instanton factors of g^{-1} have been lost).



11. The three $\mathcal{O}(\alpha_w^2)$ multiplicative corrections to Fig. 9



12. The $\mathcal{O}(\alpha_W)$ contributions in the effective action approach. Thick blob vertices come from the effective interaction, Eq. (15).



13. The $\mathcal{O}(\alpha_W^2)$ contributions in the effective action approach. Diagrams with only one blob are necessarily sub-exponential and are not shown.